STATUS OF J-PARC COMMISSIONING

Hideaki Hotchi*, 1) for J-PARC commissioning team1), 2),
1)Japan Atomic Energy Agency (JAEA), Tokai, Naka, Ibaraki, 319-1195 Japan,
2)High Energy Accelerator Research Organization (KEK), Tsukuba, Ibaraki, 305-0801 Japan

Abstract

The Japan Proton Accelerator Research Complex (J-PARC) consists of a 400-MeV linac, a 3-GeV rapid cycling synchrotron (RCS), a 50-GeV main ring synchrotron (MR) and several experimental facilities (a materials and life science experimental facility; MLF, a hadron experimental hall, and an neutrino beam line to Kamioka). The J-PARC has been beam commissioned since November 2006 and it has well proceeded as planned from the linac to the downstream facilities, the RCS and then the MR and MLF so far. In this paper, first, the current status of the linac and MR are briefly summarized, and then the commissioning results and beam performance of the RCS obtained by the end of June 2008 will be presented in more details.

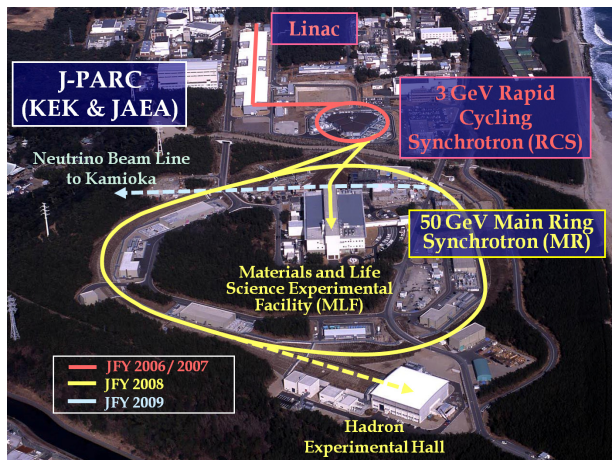

Figure 1: Bird's eye view of the J-PARC.

INTRODUCTION

The Japan Proton Accelerator Research Complex (J-PARC) located on the campus of Japan Atomic Energy Agency (JAEA) in Tokai, Naka, Japan is a multi-purpose proton accelerator facility aiming at MW-class output beam power, which was formed by jointing the neutron science project of JAEA and the hadron facility project of High Energy Accelerator Research Organization (KEK). As shown in Figure 1, the J-PARC accelerator complex [1] comprises a 400-MeV linac, a 3-GeV rapid cycling synchrotron (RCS), a 50-GeV main ring synchrotron (MR) and several experimental facilities (a materials and life science experimental facility; MLF, a hadron experimental hall, and an neutrino beam line to Kamioka).

The front-end system of the linac consists of a volume type H^- ion-source with 30 mA peak current, a radio-frequency quadrupole (RFQ) with 3 MeV output energy and a medium energy beam transport line (MEBT) for chopping and matching the 3 MeV beam to the linac. The linear accelerator consists of a drift tube linac (DTL) with 50 MeV output energy, a separated-type drift tube linac (SDTL) with 191 MeV output energy and an annular coupled structure linac (ACS) with 400 MeV output energy. So far, all the components except the ACS section have been installed to the tunnel. At present, the last two SDTL tanks are temporally installed in a linac-to-3-GeV beam transport line (L3BT) and utilized as debunchers. The output energy of the linac is 181 MeV until the ACS is installed. At full capability in the current configuration, the linac will produce 36 kW output at 181 MeV with 25 mA peak, 0.5 msec long and 53% chopper beam-on duty factor at 25 Hz repetition, which corresponds to 0.6 MW output at the RCS. The upgrade of the front-end system to get 50 mA peak current as well as the installation of the ACS for the energy recovery to 400 MeV are essential to achieve our final goal of 1 MW output at the RCS, which will be performed in the future.

The linac beam is delivered through L3BT to the RCS injection point, where it is multi-turn charge-exchange injected with a carbon stripper foil. The RCS accelerates the injected beam up to 3 GeV with 25 Hz repetition. The current injection energy is 181 MeV, for which the RCS will first aim at 0.3 - 0.6 MW output, and then drive for 1 MW output after upgrading the linac. The 3 GeV beam from the RCS is mainly transported via a 3-GeV-to-neutron-target beam transport line (3NBT) to the MLF and utilized to produce pulsed spallation neutrons and muons.

A part of the RCS beam, typically 4 pulses every 3.64 sec are transported via a 3-GeV-to-50-GeV beam transport line (3-50BT) to the MR. The MR still accelerates the injected beam to 30 GeV, delivering it to the hadron experimental hall by slow extraction and to the neutrino beam line by fast extraction. The output energy at the MR will be upgraded to 50 GeV in the second phase of the J-PARC project.

The J-PARC beam parameters are summarized in [1].

Figure 2 shows a timeline of the J-PARC commissioning. The beam commissioning began in November 2006 and has well proceeded as planned so far. We had 17 running periods in total until the scheduled summer shutdown in 2008. A typical run cycle consists of two- or three-week beam operation with one-week interval. The linac and RCS have completed initial tunings of their basic parameters in February 2008, and then since May 2008 the RCS beam has been supplied within 4 kW output to succeeding MR and MLF for their beam commissioning. The MR is now in the middle of the initial beam tuning phase started with

* hotchi.hideaki@jaea.go.jp

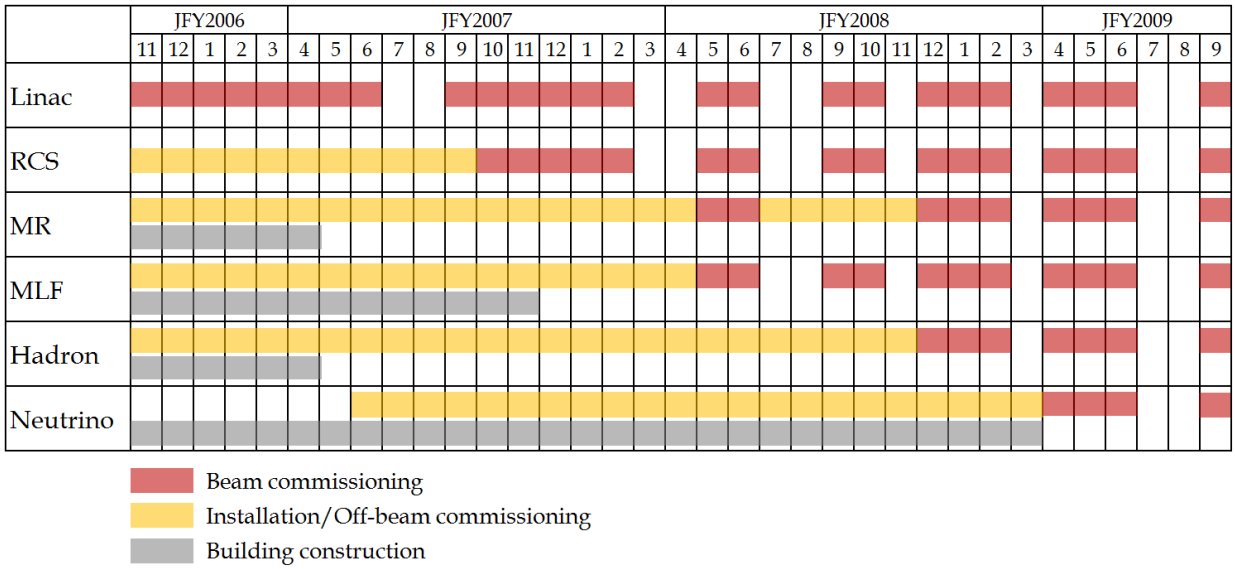

Figure 2: Timeline of the J-PARC commissioning.

the beam storage mode at the injection energy, while the linac and RCS is in transition from commissioning to the next tuning phase toward high power operations.

STATUS OF LINAC AND MR

As the current status of the linac and MR are mentioned in [2][3] in details, we will give a brief summary here.

Linac

The linac was commissioned in November 2006, and successfully accomplished 181 MeV acceleration on January 24, 2007. Discrete eight running periods through June 2007 were dedicated to commissioning the linac, for which initial beam tunings to secure a beam quality required for the coming RCS commissioning were completed. Since October 2007 after the scheduled summer shutdown in 2007, the linac beam has been successfully delivered to the RCS. Since then, the linac had nine runs until the scheduled summer shutdown in 2008. While, in the running periods, the linac focused on providing a stable beam for commissioning first the RCS and then the MR and MLF, further beam tunings for higher current operations were also continued according as a progress of the RCS commissioning.

So far the linac has performed various demonstrations with different beam conditions such as a high peak current (25 mA) operation, a long pulse (0.5 ms) operation and a high repetition (25 Hz) operation, in which the highest output beam power achieved so far is 3.5 kW at 181 MeV (25 mA peak, 0.12 ms long and 26% chopper beam-on duty factor at 25 Hz repetition) corresponding to almost 10% of the current design output. During such demonstrations, no any problem was observed such as unexpected beam losses, and deteriorations of vacuum and RF faults.

The stability and availability of the linac beam is one of key issues for efficiently commissioning the downstream facilities. The short-term beam monitoring shows an excellent stability. The energy and beam position jitters monitored over several hours were less than 20 keV (rms) and 60 μm (rms) at the RCS injection including the intrinsic jitters of the monitor system. As to the long-term beam stability, we have not still had enough data, since the downstream facilities are still in the commissioning phase and the beam conditions, especially chopper conditions, often changed according to their study items. But in the coming running period in September 2008, we plan to partly begin a 24-hour stable beam operation for the neutron target, for which sufficient data will be accumulated. In the last running period in June 2008, the availability of the linac was analyzed. The unscheduled downtime (16.6 hours) for this period was 6.4% of the total beam-on time (259 hours for 19 days), where only faults longer than one minute was analyzed and most of the downtime (12 hours) was due to a breakdown of the ion-source filament.

The linac is now stably operated with high availability and strongly backs up the commissioning of the downstream facilities.

MR

The MR was commissioned in May 2008 and smoothly achieved a beam circulation at the injection energy with a RF capture on May 22, 2008. So far the MR had discrete two beam runs until the scheduled summer shutdown in 2008 (for which beam times were shared with the MR and MLF), for which initial beam tunings, such as COD corrections and optics measurements, were successfully begun in the beam storage mode at the injection energy.

The MR has no beam till the beginning of December 2008, and dedicates this period to the installation and system commissioning of the fast and slow extraction components and also to the tuning of the main magnet power supplies. The first trial of 30 GeV acceleration is planned in December 2008.

OUTLINE OF RCS COMMISSIONING

The RCS was commissioned in October 2007 and successfully accomplished 3 GeV acceleration on October 31, 2007. Discrete six running periods through February 2008 were dedicated to commissioning the RCS, for which initial beam tunings and lots of data taking necessary for estimating a basic performance of the RCS were completed. Then since May 2008 the RCS beam has been delivered to succeeding MR and MLF for their beam commissioning. While since then the priority has been given to their beam studies, the RCS also continues necessary beam tunings and studies aiming at higher power operations.

Beam condition and injection scheme employed in the initial beam tuning phase

Most of the initial stage of the RCS commissioning was performed with low-power and low-duty operations enough that beam losses were not concern; single bunch (harmonic number h=2), 4.2×10^{11} protons per bunch and beam-on-demand operations (two bunches for h=2, 4.2×10^{13} protons per bunch and 25 Hz repetition in the design operation).

As to the injection scheme in the initial beam tuning stage, a simple center injection was employed, while the RCS adopts a painting injection scheme for both transverse and longitudinal planes to control the charge density of high power beams.

RCS operation modes

Our beam tuning scenario comprises following four operation modes; (i) injection beam dump mode, (ii) single-pass extraction mode, (iii) beam storage mode and (iv) acceleration mode.

In the injection area, three types of carbon stripper foils are installed. The 1st one is the main stripper foil utilized for the charge-exchange injection for H^- from the linac. The 2nd and 3rd ones are used for charge-exchanging H^0 and H^- unstripped on the 1st foil and delivering them to the injection beam dump. In the injection beam dump mode (i), the 1st foil is removed and the linac beam is delivered to the injection beam dump. In the injection area of the RCS, two sets of beam position monitors (BPM) and six sets of multi-wire profile monitors (MWPM) are installed. The tunings of injection and dump line orbits and also the evaluation of Twiss parameters at the injection point were performed with these monitors in this mode.

In the single-pass extraction mode (ii), the injected beam is immediately extracted with no circulation as of passing through one third of the RCS circumference and driven to the extraction beam dump. This mode was utilized for roughly checking a matching between the ring dipole magnetic field strength and the injection beam momentum in the beginning of the beam commissioning, and also for the orbit tuning and transverse matching of the linac beam.

In the beam storage mode (iii), the RCS is operated like a storage ring at the injection energy. Our beam tuning scenario is to first tune up the basic ring parameters such as optics in the beam storage mode and then to step to the acceleration mode (iv). Therefore more than half of the total beam study period assigned for the RCS so far was used for the beam storage mode.

In the following sections, beam commissioning results especially obtained in the beam storage and acceleration modes are described following the actual beam tuning procedure.

BEAM STORAGE MODE

In the beam storage mode, at first, the ring dipole magnetic field strength was matched to the injection beam momentum by looking at closed orbit displacements at dispersive arc sections. Then the revolution frequency was measured and the beam was RF captured.

Closed orbit correction

After that, the closed orbit correction was performed. Figure 3 shows closed orbit distortions (COD) measured with 54 sets of ring BPM's before and after the COD correction by 52 sets of steering magnets. While COD was observed to be around 10 mm at maximum, it was well corrected to be less than 2 mm within a few iterations by using a singular value decomposition solver for a model-based response matrix of closed orbit positions on BPM's vs. kick angles of steering magnets.

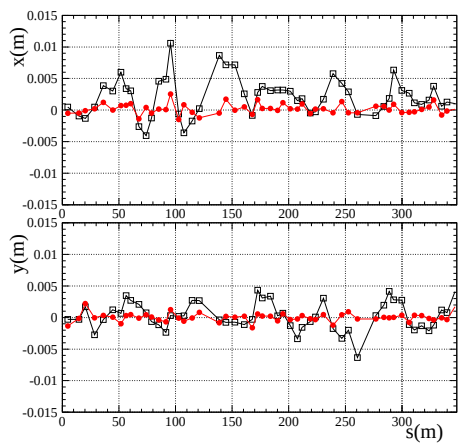

Figure 3: Horizontal (upper) and vertical (lower) COD measured in the beam storage mode before (boxes) and after (circles) the correction.

Optics measurement and its correction

Then a series of optics measurement was performed. Figure 4 shows dispersion and betatron amplitude functions obtained in the first measurement. The dispersion function was evaluated by looking at a RF frequency dependence of the closed orbit, while the betatron amplitude function

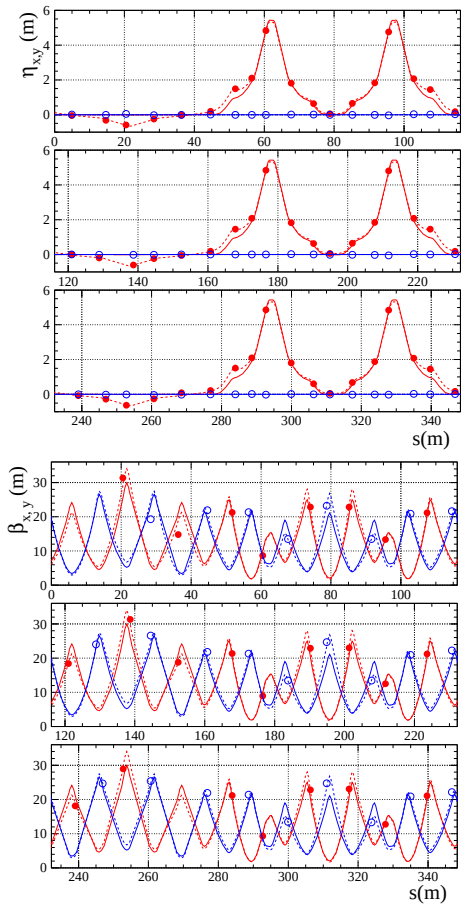

Figure 4: Dispersion (upper) and betatron amplitude (lower) functions observed in the first measurement in the beam storage mode, where the closed circles are horizontal ones and the open circles the vertical ones. The dotted curves show reconstructed optical functions in our calculation model, while the solid ones the design.

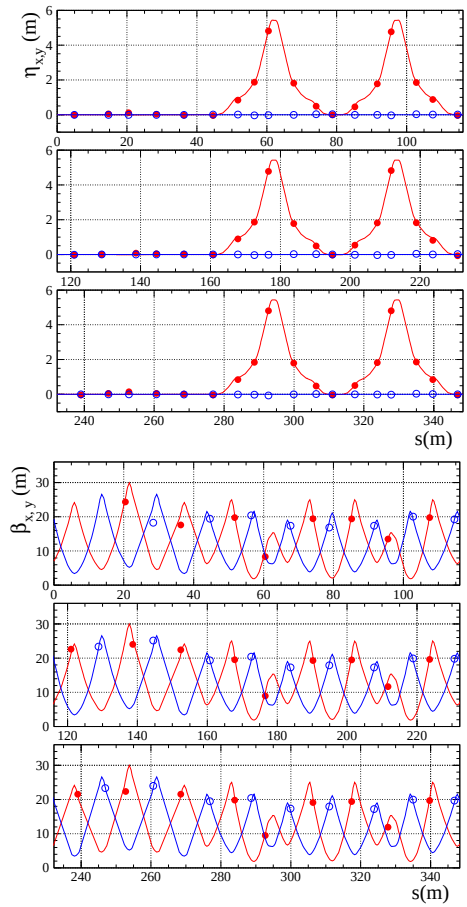

Figure 5: Corrected dispersion (upper) and betatron amplitude (lower) functions observed in the beam storage mode, where the closed circles are horizontal ones, the open circles the vertical ones, and the solid curves the design.

was estimated from a closed orbit response for a kick angle of each steering magnet. Since the ring BPM is installed inside of the steering magnet and the betatron phase difference between them is negligible, the betatron amplitude function at each steering magnet can be evaluated via a simple formula as a function of observable closed orbit response and betatron tune. While the optical functions, betatron tunes, and dispersion and betatron amplitude functions independently measured were slightly shifted from the set ones, they were well reconstructed in a unified view (dotted curves in Figure 4) in our calculation model based on the SAD [4], by which it was confirmed that a series of optics measurement was successfully performed. This model fitting in the least-square method fed fudge factors for seven families of quadrupole magnets, which compensated the gap of the set and measured optical functions, namely differences between the quadrupole strengths which gave the design optics system (solid curves in Figure 4) and the ones which reconstructed the measured optical functions (dotted curves in Figure 4). As shown in Figure 5, the optics system was successfully corrected by the fudge factors with no iteration.

Chromaticity measurement and its correction

After that, the chromaticity was estimated by looking at a RF frequency dependence of the betatron tune. The natural chromaticity was measured to be $-10.3/-7.2$ for horizontal and vertical. The RCS magnet has a large gap and an nonlinear behavior of its edge field plays a significant role. Our calculation model in which such a field nonlinearity based on the field measurement is included [5] gives a consistent magnitude of $-10.4/-6.8$, while it is $-8.5/-8.1$ if using a simple model with only linear property. The chromaticity correction was also successfully performed with field strengths of three families of sextupole magnets determined by the calculation model. Figure 6 shows chromaticity measured before and after the correction.

Injection error correction

Then finally, residual injection errors, namely betatron oscillations caused by an offset relative to the closed orbit were corrected, for which single short pulse injections, where the beam from the ion source was chopped to make a single turn (typically 560 ns bunch length), were performed to clearly catch a betatron oscillation. In this tuning procedure, turn-by-turn beam position data on two sets of BPM's

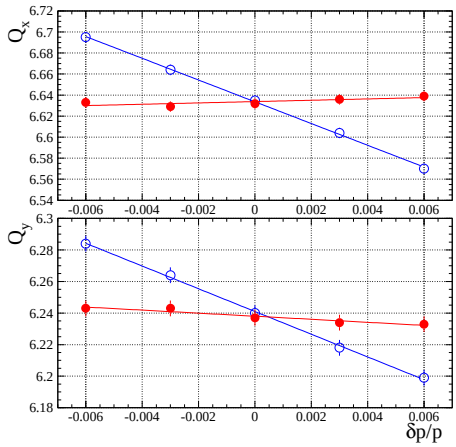

Figure 6: Horizontal (upper) and vertical (lower) chromaticity measured in the beam storage mode before (open circles) and after (closed circles) the correction.

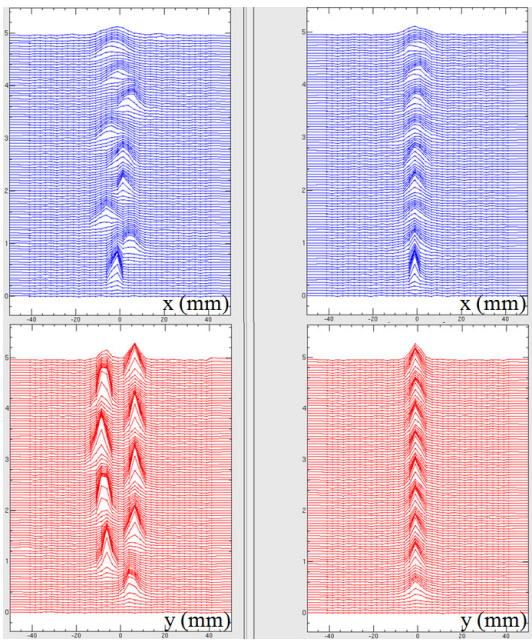

Figure 7: Horizontal (upper) and vertical (lower) beam profile mountain views for the first nine turns measured with IPM before (left) and after (right) the injection error correction.

located at the drift space in the ring were utilized to identify the phase space coordinates (position and angle) of the injection beam at the 1st stripper foil [6]. The phase space coordinates measured at the BPM pair were transferred to the injection point by a transfer matrix obtained by fitting the measured optics with our calculation model. The measured injection errors were well corrected within a few iterations using a model-based or a measured response matrix of injection beam orbits vs. field strengths of the injection line magnets. Figure 7 shows beam profile mountain views measured by ionization profile monitors (IPM) before and after the correction.

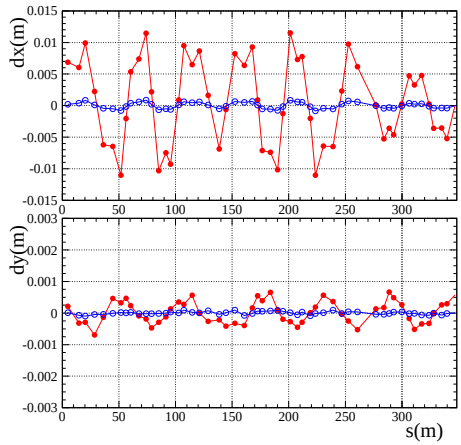

Figure 8: Horizontal (upper) and vertical (lower) COD caused by a leakage field from the DC extraction septa excited at 181 MeV (open circles) and at 3 GeV (closed circles), measured in the 181 MeV beam storage mode.

Effects of static leakage fields and tune surveys

As shown in Figure 10, the COD before the correction observed in the 3 GeV acceleration mode gradually gets smaller as accelerated, which implies that static magnetic fields from DC-excited magnets located in the extraction line leak to the ring. The RCS extraction system consists of eight sets of pulse kickers and three sets of DC septum magnets. Figure 8 shows COD caused by a leakage field from the extraction septa excited at 181 MeV and at 3 GeV, measured in the 181 MeV beam storage mode; it is a difference of COD's observed when turning the septa on (at 181 MeV or 3 GeV) and off. As shown in the figure, the leakage field is more significant when the septa are excited at 3 GeV, which makes COD of 12 mm/0.8 mm for horizontal and vertical. The magnitude of the leakage field was evaluated to be 1.4×10^{-3} Tm/0.9×10^{-4} Tm for normal and skew dipole components by fitting the measured COD distribution assuming field error sources at the extraction area. The leakage field measurement [7] was also performed, which gave a consistent magnitude of 1.7×10^{-3} Tm (normal). Similar results were obtained also for a leakage from DC magnets located in 3NBT; 1.8×10^{-3} Tm (normal)/1.6×10^{-4} Tm (skew) from the COD analysis and 1.9×10^{-3} Tm (normal) from the field measurement. Since COD caused by a leakage field can be corrected by steering magnets, the COD itself will not lead to serious problems. However, in general, such a leakage field includes higher order field components such as a quadrupole component, and can distort a superperiodicity of accelerator, additionally exciting several betatron resonances.

For this concern, betatron tune surveys were performed in the beam storage mode. Figure 9 shows beam survivals as a function of the betatron tune; the circles are the result when the extraction DC magnets are excited at 181 MeV, while the boxes are that excited at 3 GeV for which the leakage fields are more significant. As shown in the figure, several betatron resonances were observed;

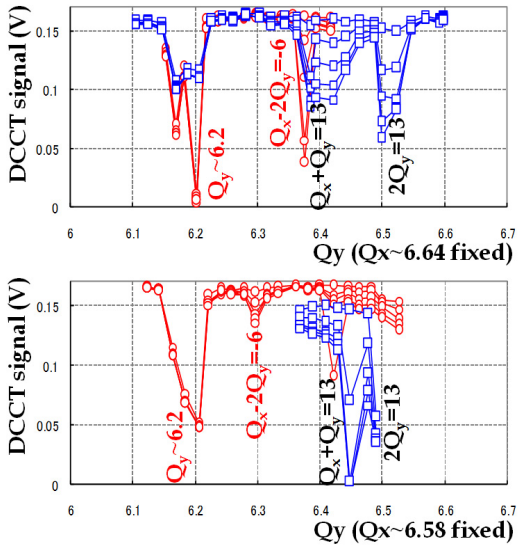

Figure 9: Beam survival as a function of the betatron tune measured in the 181 MeV beam storage mode when the extraction DC magnets were excited at 181 MeV (circles) and at 3 GeV (boxes).

half integer resonance $2Q_y$=13 and linear coupling sum resonance Q_x+Q_y=13, and 3rd order structure resonance Q_x-2Q_y=−6 from the chromaticity correction sextupoles. This figure shows the leakage fields enhance the half integer and linear coupling resonances, which means there exist significant normal and skew quadrupole components in the leakage fields. For this concern, we plan to install additional shields to get one-order of magnitude smaller leakage than the current one.

ACCELERATION MODE

We went about a tuning for the acceleration mode via the basic parameter tuning in the beam storage mode.

The RCS focusing structure consists of 24 dipole magnets (1 family; called BM) and 60 quadrupole magnets (7 family; called QFL, QDL, QFM, QDX, QFN, QDN and QFX, where QF and QD mean horizontally and vertically focusing quadrupoles), which are excited with a 25 Hz DC-biased sinusoidal current pattern in eight independent resonant networks. Also in the acceleration mode, at first, the strength at the bottom (at the injection) of the ring dipole magnetic field pattern was fitted to the injection energy.

RF frequency and closed orbit corrections over the acceleration cycle

Then the RF frequency and COD over the acceleration period (20 ms) were corrected. As already mentioned, COD's from different sources, such as COD caused by static leakage fields (variable as accelerated) and COD caused by field and alignment errors (almost constant over the revolution), were separately measured in the beam storage mode. Using such data, the steering magnetic field patterns for the acceleration were made in advance, with

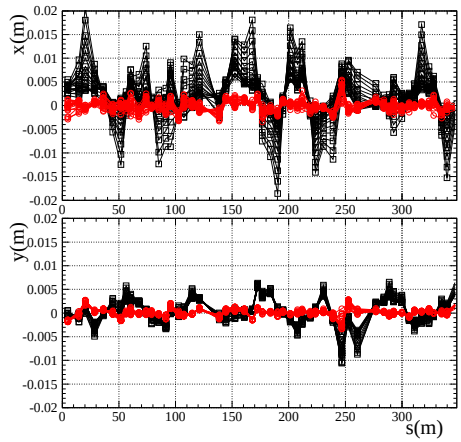

Figure 10: Horizontal (upper) and vertical (lower) COD measured over the acceleration process (20 ms) before (boxes) and after (circles) the COD correction.

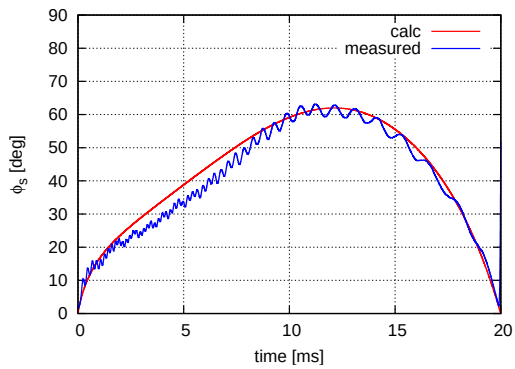

Figure 11: Synchronous phase measured over the acceleration time; the blue curve is the measured one, while the red curve the calculated one assuming that the RF voltage is a pure sine-wave.

which COD over the acceleration time was roughly corrected from the beginning of the tuning in the acceleration mode. Under such a situation, the RF frequency was first corrected so as to minimize a deviation of the horizontal closed orbit especially in the dispersive arc sections caused by a mismatch to the dipole field pattern, and then residual COD was corrected by modifying the steering field patterns. In this way, the effects for transverse and longitudinal motions were separately well compensated. Figure 10 shows COD observed over the acceleration process without and with the COD correction by the steering magnets. As shown by circles, it was well corrected to be a few mm over the revolution.

Synchronous phase

Figure 11 shows a synchronous phase (ϕ_s) measured over the acceleration time, where the blue curve shows the measured one, and the red curve the calculated one assuming that the RF voltage is a pure sine-wave. They are in good agreement, by which it was confirmed that the RF voltages set and actually felt by the beam were consistent with each other [8]. The slight difference from 3 ms to 7

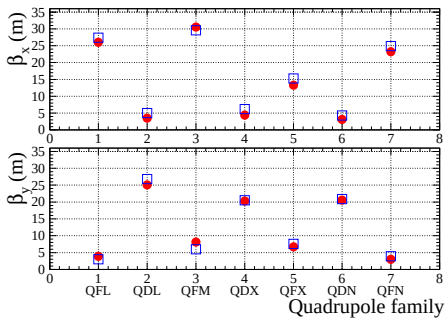

Figure 12: Averaged betatron amplitude function for each quadrupole family in the horizontal (upper) and vertical (lower) planes; the circles are the result measured at the bottom of the acceleration pattern, while the boxes are that for the beam storage mode.

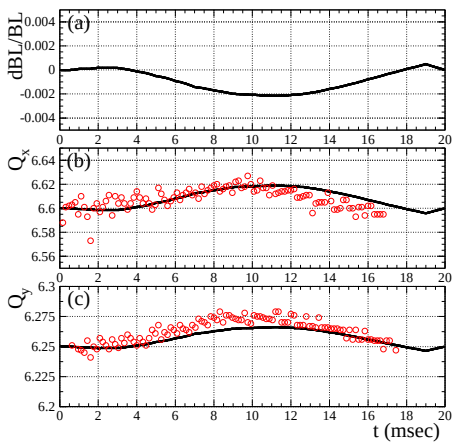

Figure 13: (a) Deviation of the main dipole field pattern from the ideal sinusoidal wave, estimated from the RF frequency pattern. (b) Horizontal tune excursion measured over the acceleration process, where the solid curve is the calculated variation assuming the deviation of (a). (c) Vertical ones.

ms is from a 3rd harmonic component intrinsic in the RF voltage. Therefore the agreement got much better by canceling the 3rd harmonic component by a counter phasing which set the odd and even ones out of 10 cavities at ± 30 degrees [8].

The longitudinal phase and profile and also the closed orbit (mentioned in the last subsection) were reproductive every cycle especially in virtue of the excellent stability of the linac energy, the ring dipole magnetic field and the RF frequency and voltage.

Optics over the acceleration cycle

After fixing the closed orbit, the betatron amplitude function at the injection was evaluated by observing betatron tune vs. strength of each quadrupole family in order to confirm the consistency among the optical properties at the bottom of the acceleration pattern and in the beam storage mode. They were in good agreement as shown in Figure 12.

Figure 13-(b) and -(c) show betatron tune excursions measured over the acceleration process, which reflect a

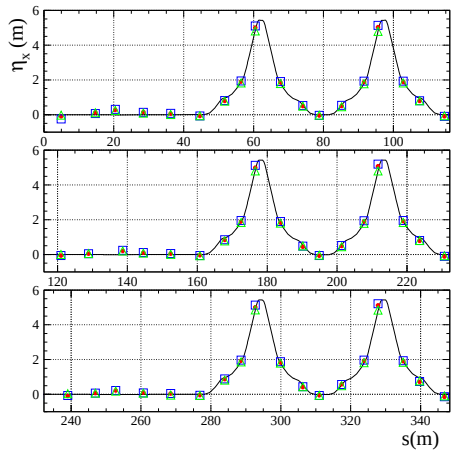

Figure 14: Horizontal dispersions measured at 12 ms (circles), 15 ms (boxes) and 18 ms (triangles) in the acceleration period (20 ms), where the solid curves are the design.

magnetic field tracking error among main dipole and quadrupole families. While the field pattern of the main dipole and quadrupole magnets is to be closely corrected to ideal sinusoidal wave form within a few $\times 10^{-4}$ by using high frequency waves, only the dipole field pattern is still slightly shifted from the ideal form by 0.2% at maximum due to the limit of its power supply capability as shown in Figure 13-(a). The solid curves in Figure 13-(b) and -(c) show calculated tune excursions assuming the deviation of the dipole field pattern. While the tendencies of the calculated and measured tune variations are very alike, there still remains a slight difference, which implies there exist slight tracking errors also among the quadrupole families. The measurements of betatron amplitude functions as well as betatron tunes over the acceleration time, which will be performed in the near future, give us more precise information on the field tracking error, leading to a closer field tracking which settles the tunes, and also its applied scheme which dynamically moves the tunes over the acceleration by adjusting DC, AC components and phase of the quadrupole field patterns. The dynamical tune control will be very useful to manage beam losses especially for higher power operations [9].

Figure 14 shows dispersion functions observed at 12 ms, 15 ms and 18 ms in the acceleration period (20 ms). They are almost consistent with that tuned up in the beam storage mode. The chromaticity was also measured over the acceleration time. At present the chromaticity correction sextupole magnets are excited with DC power supplies and the chromaticity is corrected at the injection energy. Therefore the chromaticity gradually recovers as accelerated. The measured result reasonably shows such a situation.

Through such a series of measurement, it was confirmed that the optics over the acceleration process adequately kept the condition determined in the beam storage mode.

High beam power demonstrations

After the initial beam tuning procedure mentioned above, we performed high power demonstrations at 25 Hz

repetition for four minutes up to the limit of the beam dump capacity (within 4 kW in 1-hour average), in which 52 kW output was successfully achieved; 1-bunch operation with 4.6×10^{12} protons per pulse using the linac beam of 25 mA peak, 0.12 ms long and 26% chopper beam-on duty factor. The demonstration was carried out with no painting injection, for which the beam loss rate was 6.5% only around the injection energy, corresponding to 200 W in power for the collimator limit of 4 kW. During the demonstration, no any trouble, such as beam instabilities, unexpected beam losses and degradations of vacuum, was observed.

In addition we demonstrated a 2-bunch operation and successfully achieved the acceleration and extraction of 1.1×10^{13} particles per pulse. No significant beam loss was observed at the extraction and the beam loss rate was similarly 6.5% only around the injection energy. While this demonstration was performed with no repetition (namely beam-on-demand operation), the output power corresponds to 130 kW if performing 25 Hz repetition. This is the maximum instantaneous output achieved so far at the RCS.

PAINTING INJECTION

We have recently performed a preliminary test of transverse and longitudinal painting injections in the beam storage mode using a long pulse with a design length of 0.5 ms (5 mA peak, 0.5 ms long and typically 26% chopper beam-on duty factor, corresponding to single-bunch operation with 4.2×10^{12} per bunch at the RCS).

For the transverse beam painting, two types of orbit-bump systems are prepared. One is the shift-bump system to make an orbit offset at the injection point, which produces a flat top field during the multi-turn injection. The other is the paint-bump system to make a time dependent bump orbit at the injection point for the beam painting. In the horizontal plane the injection beam was painted from inside to outside of the RCS beam ellipse in the phase space by shifting the closed orbit, while in the vertical plane the injection beam was moved from inside to outside or from outside to inside. A series of tuning procedure for the painting, such as identifying injection-beam phase-space coordinates relative to the closed orbit at the injection point over the beam painting process and changing the painting area, was successfully demonstrated in the beam storage mode [6][10]. Figure 15 shows beam profile mountain views measured with IPM for the beam painting of 100π mm mrad (216π mm mrad in the design).

On the other hand, the longitudinal beam painting was performed by combination of the momentum-offset injection scheme, in which the RF frequency had an offset, and superposing a 2nd harmonic RF voltage to widen and flatten the RF bucket. The phase sweep of the 2nd harmonic RF voltage relative to the fundamental one was also employed so that the shape of the RF bucket was dynamically changed through the injection process. For improving a degradation of the bunching factor, the longitudinal motion was surveyed for various parameters [11] preliminarily in the beam storage mode. Figure 16 shows longitudinal beam profile mountain views measured with a wall current monitor (WCM) without and with the longitudinal painting, where the 2nd harmonic component with amplitude of 80% for that of the fundamental voltage, its phase sweeping from -60 to 0 degrees and the RF frequency offset corresponding to -0.2% momentum offset were employed for the beam painting. The figure clearly shows the effectiveness of the momentum offset and the superposition and phase sweeping of the 2nd harmonic component.

While the painting injection scheme is very effective to

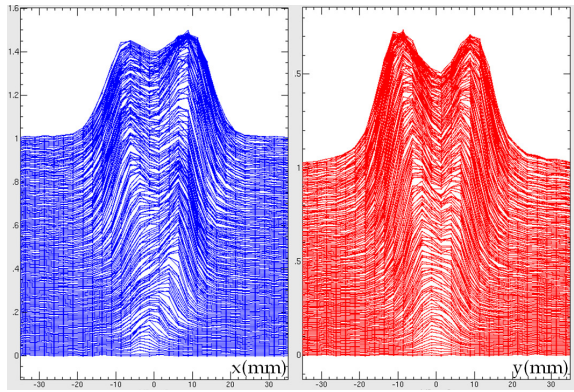

Figure 15: Horizontal (left) and vertical (right) beam profile mountain views for the injection period (0.5 ms) measured with IPM for the transverse beam painting of 100π mm mrad, where the injection beam was painted from inside to outside of the RCS beam ellipse in the phase space for both horizontal and vertical.

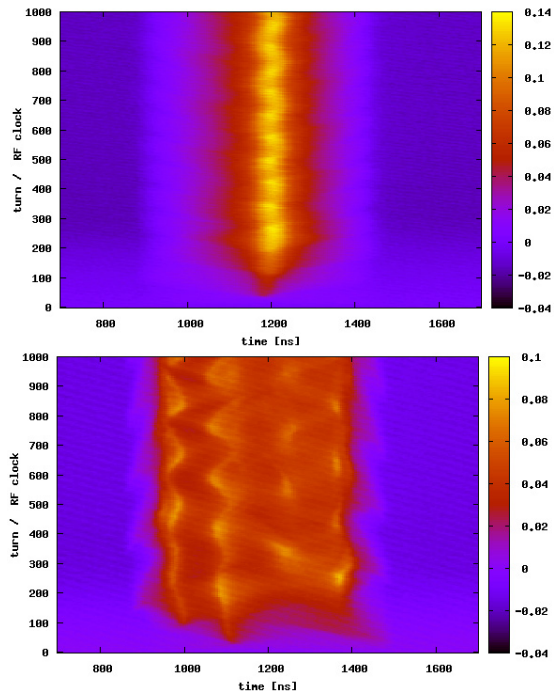

Figure 16: Longitudinal beam profile mountain views for the injection period (0.5 ms) measured with WCM without (upper) and with (lower) the longitudinal beam painting.

control the charge density of the beam, it increases particles with large amplitudes for both transverse and longitudinal planes, and possibly causes some issues by their nonlinear behavior. In order to gain the sufficient ability of the painting injection, it is essential to fulfill the global optimization for various parameters complicatedly intertwined with each other; the search of the bare working tune having a dynamic aperture large enough for the transverse painting area, the optimization of the tune variation to keep the beam stable over the revolution considering the bare working point set at the injection and the magnitude and footprint of the space-charge tune shift, the balance of the transverse and longitudinal painting areas and so on. In the next running period in September 2008, we will try such a optimization procedure using a high intensity beam with 200 kW output or more.

RESIDUAL RADIATIONS OF RCS

Residual radiation surveys for the accelerator components have been performed after every beam run, where the radiation level is measured with contact on vacuum chamber typically half day after the beam shutdown. Here we show a result of the residual radiation survey performed after the run period in February 2008 for which the high power demonstration, mentioned in the last section, was performed.

The highest level was detected to be 120 μSv/h at the entrance of the collimator section located just downstream of the injection area. As to the injection area, the radiation level was around 16 μSv/h or less, where there are many possible sources of particle losses such as Lorentz stripping, H0 excitation and foil scattering. The most significant beam loss source at the injection is the scattering on the 1st stripper carbon foil. At present, the center injection is typically performed, and the present falling time of the injection orbit bump (500 μsec) is longer than the design time (180 μsec). In addition, the size of the 1st stripper foil is still larger than a proper size. These situations increase the frequency of the foil scattering; it is eight times larger than the design and its resultant beam loss rate is estimated to be 1.5% [6][12]. Most of the lost particles should be localized on the collimator, but some of them with large scattering angles lead to uncontrolled beam losses just downstream of the injection section. The radiations mentioned above probably come from such a particle loss.

While also at the locations with large dispersion, some radiations, 3.5 - 12 μSv/h, were detected, they probably come from beam losses during the RF tuning and the longitudinal studies. As to the extraction section, no significant radiation was detected.

At present, there is no significant machine activation and it looks particle losses are almost localized on the collimators [13]. However we have not still had enough data on the machine activation for continuous beam operations, because so far low-duty and beam-on-demand operations have typically been employed for the RCS. We hereafter need to still more carefully monitor the trend of the residual radiation level, as the continuous beam operation for the MLF begins in September 2008.

PROSPECT OF J-PARC COMMISSIONING

The schedule of the J-PARC beam commissioning in the next one year is summarized here.

Now we are in the scheduled summer shutdown. The beam test will be re-started in September 2008. In September and October, only the linac and RCS have beam runs, for which, first, we will take the government inspection for the MLF and then continuous beam operations within 4 kW output at 3 GeV are planned for the MLF. In this period, high power demonstrations with 200 kW output or more at 3 GeV will be also performed with the painting injection.

The MR has no beam through the beginning of December 2008, and dedicates this period to the installation and system commissioning of the fast and slow extraction components and also to the tuning of the main magnet power supplies. As to one month in November, the installation and system commissioning of the 11th RF cavity are also planned at the RCS, and thus the J-PARC have no beam for this period.

Then in December 2008 we will try the acceleration to 30 GeV and also the fast and slow extractions at the MR. User runs will also start at the MLF in December with first 4 kW beam and then hopefully 100 kW. Then the MR will start to deliver the beam to the hadron experimental hall in February 2009 and then to the neutrino beam line in April.

SUMMARY

The J-PARC has been commissioned since November 2006. The linac and RCS have completed initial tunings of their basic parameters in February 2008, and then since May 2008 the RCS beam has been supplied to succeeding MR and MLF for their beam commissioning. The linac and RCS is now in transition from commissioning to operation, and our efforts hereafter will be focused on high power operations introducing the beam painting scheme. On the other hand, the MR is now in the middle of the initial tuning phase started with the beam storage mode at the injection energy. The J-PARC beam commissioning has steadily proceeded as planned so far.

REFERENCES

[1] Y. Yamazaki ed., “Accelerator Technical Design Report for High-Intensity Proton Accelerator Facility Project”, JAERI-Tech 2003-044 and KEK Report 2002-13.

[2] M. Ikegami, “Transition from Commissioning to Operation in the J-PARC Linac” and “Measurement and Simulations of the J-PARC Linac”, Proc. of HB2008 Workshop, Nashville, Tennessee, August 25-29, 2008.

[3] T. Koseki, "Beam Commissioning of J-PARC MR", Proc. of HB2008 Workshop, Nashville, Tennessee, August 25-29, 2008.

[4] http://acc-physics.kek.jp/SAD/sad.html.

[5] H. Hotchi *et al.*, "Evaluation of Nonlinear Effects in the 3-GeV Rapid Cycling Synchrotron of J-PARC", Proc. of PAC2005 Conference, Knoxville, Tennessee, May 16-20, 2005., p.916.; H. Hotchi *et al.*, "Effects of Intrinsic Nonlinear Fields in the J-PARC RCS", Proc. of EPAC2006 Conference, Edinburgh, UK, June 26-30, 2006., p.2104.

[6] P. K. Saha, "Experience with J-PARC RCS Injection and Extraction Systems", Proc. of HB2008 Workshop, Nashville, Tennessee, August 25-29, 2008.

[7] M. Yoshimoto *et al.*, "Leakage Field of Septum Magnets of 3-GeV RCS at J-PARC", Proc. of EPAC2008 Conference, Genoa, Italy, June 23-27, 2008, p.3626.

[8] F. Tamura *et al.*, "Beam Acceleration with Full-Digital LLRF Control System in the J-PARC RCS", Proc. of EPAC2008 Conference, Genoa, Italy, June 23-27, 2008, p.364.

[9] H. Hotchi *et al.*, "Effects of Magnetic Field Tracking Errors on Beam Dynamics at J-PARC RCS", Proc. of PAC2007 Conference, Albuquerque, New Mexico, June 25-29, 2007, p.4078.

[10] H. Harada, Ph.D. thesis, Hiroshima University, 2009, to be published.

[11] M. Yamamoto *et al.*, "Longitudinal Particle Simulation for J-PARC RCS", Proc. of 5th Annual Meetings of Particle Accelerator Society of Japan, 2005.

[12] P. K. Saha *et al.*, "Updated Simulation for the Nuclear Scattering Loss Estimation at the RCS Injection Area", Proc. of PAC2007 Conference, Albuquerque, New Mexico, June 25-29, 2007., p.1526.

[13] K. Yamamoto, "J-PARC Collimation System Experience", Proc. of HB2008 Workshop, Nashville, Tennessee, August 25-29, 2008.